# Origin of Poor Cyclability in Li2NInSiO4 from First-Principles Calculations: Layer Exfoliation and Unstable Cycled Structure

**ARTICLE** *in* CHEMISTRY OF MATERIALS · JUNE 2014

Impact Factor: 8.35 · DOI: 10.1021/cm500803e

CHEMISTRY OF MATERIALS

Article

pubs.acs.org/cm

# Origin of Poor Cyclability in $Li_2MnSiO_4$ from First-Principles Calculations: Layer Exfoliation and Unstable Cycled Structure

Hosik Lee,[†] Soon-Dong Park,[†] Janghyuk Moon,[‡] Hoonkyung Lee,[§] Kyeongjae Cho,[‡] Maenghyo Cho,[‡] and Sung Youb Kim*,[†]

[†]School of Mechanical and Nuclear Engineering, Ulsan National Institute of Science and Technology (UNIST), Ulsan 689-798, South Korea

[‡]School of Mechanical and Aerospace Engineering, Seoul National University, Seoul 151-744, South Korea

[§]School of Physics, Konkuk University, Seoul 143-701, South Korea

**ABSTRACT:** Good cyclability is essential for the potential application of cathode materials. Here, we investigate the structural stability of two-dimensional (2D) Li-layered and three-dimensional (3D) structured polymorphs of $Li_2FeSiO_4$ and $Li_2MnSiO_4$ using the density functional theory calculations. We find that all 2D Li-layered polymorphs of both materials are unstable upon full delithiation owing to layer exfoliation, which can lead to an amorphous structure. However, in contrast to the fact that the amorphization of $Li_2FeSiO_4$ can be prevented by the formation of the 3D cycled structure that is energetically stable, the 3D cycled structure of $Li_2MnSiO_4$ is found to be unstable during delithiationlithiation cycling. As a result, $Li_2MnSiO_4$ easily undergoes amorphization and shows a poor cyclability.

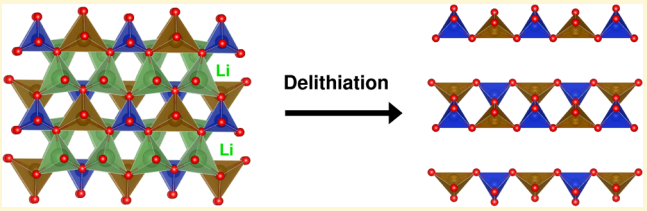


## INTRODUCTION

Lithium transition-metal silicates, $Li_2MSiO_4$ (M = Fe, Mn), have been the subject of intensive studies as a potential cathode of lithium-ion batteries because of high theoretical capacities, environmental friendliness, thermal stability, and inexpensiveness.[1−19] In particular, the high theoretical capacity of ∼330 mAh/g by the utilization of two lithium ions per formula unit is the most attractive aspect in materials research for a cathode.[2] During the charging−discharging process that corresponds to the delithiation−lithiation of the materials, reversibility of the structure and voltage stability are required for the good cyclability. Flat voltage region in the charge−discharge profile indicates directly the voltage stability and give indirect information on the reversibility of structures. The flat voltage region that is sustained upon charging−discharging cyclings shows the reversibility of the structures and the shift of the flat voltage position indicate a structural phase transition to a different polymorph. In experiments, $Li_2FeSiO_4$ polymorphs exhibit good cyclability with the utilization of one lithium ion per formula unit[1,13] and the ∼0.3 V lowering of the flat voltage position during cyclings is observed at the beginning of cycling.[4,13] With experimental structure identifications and computational simulations, the voltage drop upon electrochemical cycling is attributed to the phase transition of the 3D cycled structure.[5−8] Compared to the other 2D Li-layered polymorphs of $Li_2FeSiO_4$, the cycled structure has a three-dimensional Li matrix caused by Li/Fe cation exchanges[4] that sustain similar Li migration barriers compared to 2D Li-layered polymorphs.[9]

However, $Li_2MnSiO_4$ polymorphs have been exhibited poor cyclability with capacity fading and the absence of a flat voltage region in the charge−discharge profile[2,3,10,20,21] although Honma et al. insists stable cyclability up to 50 cycles.[10,11,22] If one can observe a flat voltage region, it can be assumed that the local environment of extracting lithium ions is unchanged and the whole structure is stable during cyclings, because the flat voltage region in the charge−discharge profile indicates that the energy difference between $Li_2MnSiO_4$ and $LiMnSiO_4$ remains constant during cyclings. In that sense, the absence of a flat voltage region may imply that $Li_2MnSiO_4$ structures can be unstable upon lithiation/delithiation.

The instability of $Li_2MnSiO_4$ polymorphs during delithiation/lithiation is suggested by previous studies.[12,18,19] With first-principles calculation results, Arroyo-de Dompablo et al. insisted that fully delithiated $MnSiO_4$ can show layer separation and structural phase transformation upon lithium removal may appear addressing $LiMnO_2$ case.[18] In experiments, the instability of $Li_2MnSiO_4$ polymorphs is supported by TEM and electron diffraction patterns that show that original and amorphous regions coexist in a sample with an average composition of half-delithiated $LiMnSiO_4$.[12] In comparison, $Li_2FeSiO_4$ polymorphs exhibit two flat voltage regions that correspond to $Fe^{2+}/Fe^{3+}$ and $Fe^{3+}/Fe^{4+}$ redox couples.[13] Considering that one of flat voltage regions corresponds to a $Li_2FeSiO_4$ 3D cycled structure (the stable structure upon lithium removal),[5−8] a question arises: Is the 3D cycled structure of $Li_2MnSiO_4$ stable? This will be a fundamental question for the application of a cathode with stable cyclability.

Received: March 6, 2014
Revised: June 12, 2014
Published: June 13, 2014

  

In this work, we investigate the stability of 2D Li-layered polymorphs as well as 3D cycled structures of $Li_2MSiO_4$ (M = Fe, Mn), including half- and full-delithiated states using first-principles calculations. As a result, we explain why $Li_2MnSiO_4$ exhibits poor cyclability in contrast to $Li_2FeSiO_4$ on the basis of energetics and calculated voltages for different structures.

## COMPUTATIONAL DETAILS

First-principles calculations were performed using density functional theory (DFT) with the generalized gradient approximation of Perdew–Burke–Ernzerhof[23] (GGA PBE) and the GGA+U approximation.[24] A plane–wave basis set with a kinetic energy cutoff of 40 Ry and ultrasoft pseudopotentials were used throughout the calculations. The Brillouin zone integration was performed with a 3 × 3 × 3 Mokhorst-Pack k-point grid.[25] The unit-cell lattice vectors (unit cell shape and size) and atomic coordinates are fully relaxed until the force on each atom is less than 0.023 eV/Å. All calculation results were ferromagnetic. Our choice for the Hubbard U parameter are $U_{Fe}$ = 4.5 eV, $U_{Mn}$ = 6.0 eV. Our values for the Hubbard U correspond to the U-J differences, where U and J denote the intrasite Coulomb and exchange interactions, respectively. Our calculation model is based on the parameters of Zhang et al.[26] The calculated voltage upon delithiation is calculated by the standard approach.[27,28]

## RESULTS AND DISCUSSION

We perform the density functional calculations with three known 2D Li-layered polymorphs of $Li_2MSiO_4$ (M = Fe, Mn) as shown in Figure 1a–c. Upon full delithiation, all polymorphs

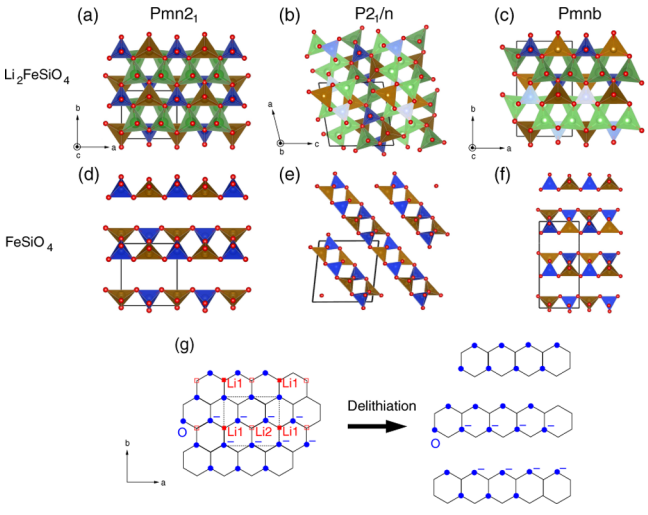


**Figure 1.** (a–f) Structures of $Li_2FeSiO_4$ and $FeSiO_4$. Red spheres indicate oxygen ions. Green, brown, and blue polyhedrons represent Li, Fe, and Si tetrahedrons, respectively. Solid boxes indicate the unit cells of the structures. Manganese silicates exhibit similar layer exfoliation. (g) Schematic description of layer exfoliation upon full delithiation.

of $MSiO_4$ (M = Fe, Mn) exhibit layer exfoliation as shown in Figure 1d–f. The calculated lattice parameters and unitcell volumes are shown with Table 1 and 2. Owing to repulsive Coulomb interactions between the oxygen anions in different layers, repulsive forces are applied to each layer. At the full and partial occupation of Li sites, attractive Coulomb forces between the Li and O ions compensate for the repulsive ones and sustain the entire structures. However, the repulsive forces at full delithiation become dominant; thus, atomic layers are exfoliated, as shown by the schematics in Figure 1g. Because of the layer exfoliations, $Li_2MSiO_4$ (M = Fe, Mn) cannot sustain

**Table 1. Calculated Lattice Parameters (in Å) and Volumes (in Å$^3$) for $Li_xFeSiO_4$ ($x$ = 0, 1, 2) Polymorphs[a]**

| $x$ | structure | $a$ | $b$ | $c$ | $\beta$ | $V$ (Å$^3$/fu) |
|---|---|---|---|---|---|---|
| 2 | $Pmn2_1$ | 6.357 | 5.462 | 5.045 | 90.00 | 87.59 |
| 1 | $Pmn2_1$ | 6.133 | 5.622 | 5.096 | 91.29 | 87.76 |
| 2 | 3D-cycled | 6.302 | 5.519 | 5.056 | 89.62 | 87.94 |
| 1 | 3D-cycled | 6.659 | 5.307 | 5.120 | 90.22 | 90.48 |
| 0 | 3D-cycled | 7.716 | 5.476 | 5.512 | 89.45 | 116.35 |

[a]3D cycled structure is denoted as 3D-cycled.

**Table 2. Calculated Lattice Parameters (in Å) and Volumes (in Å$^3$) for $Li_xMnSiO_4$ ($x$ = 0, 1, 2) Polymorphs[a]**

| $x$ | structure | $a$ | $b$ | $c$ | $\gamma$ | $V$ (Å$^3$/fu) |
|---|---|---|---|---|---|---|
| 2 | $Pmn2_1$ | 6.468 | 5.429 | 5.039 | 90.00 | 88.48 |
| 1 | $Pmn2_1$ | 6.473 | 5.670 | 5.354 | 56.73 | 82.15 |
| 2 | 3D-cycled | 7.730 | 5.467 | 5.065 | 90.27 | 107.01 |
| 1 | 3D-cycled | 7.988 | 5.775 | 5.490 | 95.93 | 125.97 |
| 0 | 3D-cycled | 7.610 | 6.022 | 5.907 | 89.70 | 134.89 |

[a]3D cycled structure is denoted as 3D-cycled.

the 2D Li-layered structures; therefore, other structures such as a cycled or amorphized structure are present during cycling. The possibility of layer exfoliation and the successive amorphization is discussed by previous workers,[18,19] and our computational results support these discussions. We stress that layer exfoliation is observed at full delithiation by the two independent simulation packages of quantum-espresso[29] and castep.[30]

For the stability study of 3D cycled structures, we consider three possible configurations by exchanging the cations of the $Pmn2_1$ structure, as shown in Figure 2a–c and Figure 2d–f for $Li_2FeSiO_4$ and $Li_2MnSiO_4$, respectively. Among them, configurations a and d are 3D structures of the Li matrix and the others contain 2D Li-layers similar to the other polymorphs in Figure 1. Because the 3D structure has remaining cations between the layers at full delithiation, the corresponding calculation results do not show the layer exfoliations and they show stability of the 3D structure during cyclings. To confirm the structural stability during cycling, we compare the energies of the 3D cycled structure at any Li content with the 2D Li-layered ($Pmn2_1$) structure in Figure 2g. The 3D cycled structure of iron silicate has lower energies at delithiated conditions and a slightly higher energy in the fully lithiated $Pmn2_1$ structure. Because the higher energy is not so large (~0.06 eV/FU), the 3D cycled structure can be sustained at cycling with low risk of amorphization. The experimental observations of higher capacity at higher temperature[13] can be explained with this small energy difference at full lithiation; because the 2D Li-layered structure has lower energy for the fully lithiated $Li_2FeSiO_4$, there is possibility of a phase transition from the 3D cycled structure to the 2D Li-layered structure. At higher temperature, the possibility of 2D Li-layered structure decreases, whereas the possibility of a 3D cycled structure increases. Therefore, the entire processes of cyclings can be performed at higher temperature without a phase transition to the 2D Li-layered structure, which leads to capacity loss with amorphization. On the contrary, the 3D structure of manganese silicate has much higher energies than the 2D Li-layered structures ($Pmn2_1$) at full lithiation as well as full delithiation; however, the 3D structure of $LiMnSiO_4$ has a lower energy than the 2D structure, as shown in Figure 2g. Therefore, manganese


dx.doi.org/10.1021/cm500803e | Chem. Mater. 2014, 26, 3896–3899

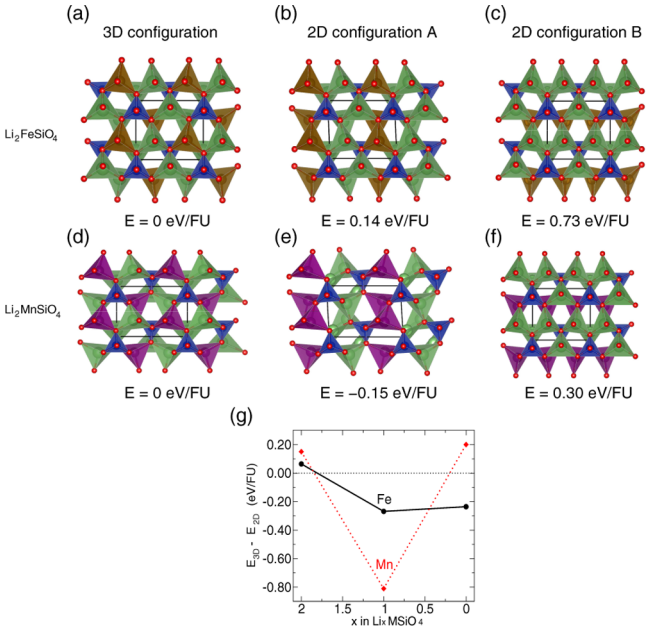


**Figure 2.** (a–f) Cation-exchanged structures of $Li_2MSiO_4$ (M = Fe, Mn) Red spheres indicate oxygen ions. Green, brown, blue, and purple polyhedrons indicate Li, Fe, Si, and Mn tetrahedrons, respectively. Solid boxes indicate the unit cells of the structures. The relative energies to the 3D configurations are shown at the bottom of each figure. (g) Relative energies of the cation exchanged structures compared to the lowest energy configuration of the 2D Li-layered structures at different Li content.

silicate can undergo the structural transition of 2D-($Li_2MnSiO_4$)-3D($LiMnSiO_4$)-2D($MnSiO_4$) on cycling on the basis of its energetics. This can be the origin of instability and poor cyclability in manganese silicates. From another point of view, the instability of maganese silicate can be related with the fact that stable coordination of Mn (3+) is not tetrahedral but distorted octahedral or square-pyramidal.[17] It is in contrast to Fe case, for stable coordination of Fe (3+) is tetrahedral. Therefore, $Mn^{2+}$ $O_4$ tetrahedron is likely to change the coordination number but $Fe^{2+}$ $O_4$ tedrahedron remains in its original form during the $M^{2+}/M^{3+}$ redox couplings of lithiation/delithiation. Note that the calculations of other polymorphs are not necessary because the 3D structure of manganese silicate has higher energies than the $Pmn2_1$-originated structures. Regardless of the other polymorphs, manganese silicate is already more unstable than the $Pmn2_1$-originating structures.

We plot the voltage-composition curves for $Li_2FeSiO_4$ and $Li_2MnSiO_4$ in panels a and b in Figure 3, respectively. Consistent with previous works,[7,8] the ∼0.3 V voltage drop of the 3D cycled structure for the $Fe^{2+}/Fe^{3+}$ redox coupling is observed. It is remarkable that the calculated voltage of the 2D Li-layered structure for the $Mn^{2+}/Mn^{3+}$ and $Mn^{3+}/Mn^{4+}$ redox couplings are similar in the case of manganese silicate. This indicates that the two redox processes do not occur sequentially but can occur simultaneously. As a result, some part of manganese silicate becomes unstable by layer exfoliations when it is fully delithiated and amorphization follows. On the contrary, the two redox couplings of iron silicate are well separated in voltage as shown in Figure 3a, which indicates that an amorphous phase is not necessary because the 3D structure is stable during cycles.

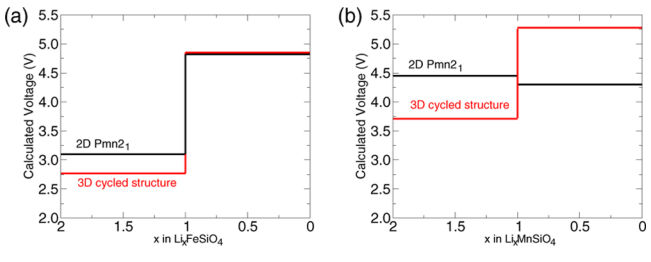


**Figure 3.** Calculated voltage–composition curves for $Li_2FeSiO_4$ and $Li_2MnSiO_4$. Those of 3D cycled structure are represented by red lines.

The recent experimental results of Honma et al.[10,11,22] seem to be inconsistent with our calculation results. In direct contradiction to our results of poor cyclability, they report a discharge capacity of ∼340 mAh/g with $Li_2MSiO_4$ nanoparticles in contact with multiwall carbon nanotubes (MWCNTs)[22] or nanoporous carbon.[10] Because of low conductivity of $Li_2MSiO_4$, carbon coating is performed in the form of MWCNTs or nanoporous carbon to increase electrical conductivity. We note that MWCNTs or porous carbon have been investigated as cathodes of Li air batteries.[31−34] Because carbon-coated $Li_2MSiO_4$ is used as a cathode material in the electrochemical cell, carbon materials like MWCNTs are common to the $Li_2MSiO_4$ and nonaqueous Li air battery cells. Moreover, the two cells adopt lithium metals as anode and the voltage in the charge–discharge profile shows a similar value. Thus, we should consider the capacity comes from the carbon materials rather than $Li_2MSiO_4$ materials. According to Chen et al.,[31] the MWCNT cathode shows a capacity of 1000 mAh/g, which is almost three times as large as the theoretical maximum capacity of $Li_2MSiO_4$. Therefore, it will be necessary to measure the corresponding contribution beside $Li_2MSiO_4$ materials. Reaction product detection of $Li_2O_2$ or LiOH may be a way to measure the contribution.

Let us discuss on the formation mechanism of 3D structures. During lithium extraction, vacancies are formed in the lithium sites. Then, Fe or Mn cations can migrate into the lithium vacancy sites with some migration barrier. Because charging voltage is more than 3 V, cations may migrate into the stable position in the delithiation/lithiation configurations. According to Armstrong et al.[5] and our computational results, there can be ordering of exchanged Fe cations because the 3D structure of $Li_2MSiO_4$ has the lowest energy within cation-exchanged structures.

## SUMMARY

In summary, we study the stability of $Li_2MSiO_4$ (M = Fe, Mn) polymorphs. We find that the 2D Li-layered polymorphs of $Li_2MSiO_4$(M = Fe, Mn) at full delithiation become unstable because of layer exfoliation and that this layer exfoliation can be prevented by the formation of a 3D cycled structure. However, the 3D cycled structure of $Li_2MnSiO_4$ is energetically unstable resulting in poor cyclability, which is in contrast to the 3D cycled structure of $Li_2FeSiO_4$ that is stable during cycling.

## AUTHOR INFORMATION

### Corresponding Author

*E-mail: sykim@unist.ac.kr.

### Notes

The authors declare no competing financial interest.

## ■ ACKNOWLEDGMENTS

This work was supported by the National Research Foundation of Korea (NRF) (Grant 2012R1A1A2043431, 2012-0029212, 10041589) and the PLSI supercomputing resources of the Korea Institute of Science and Technology Information.

## ■ REFERENCES

(1) Nytén, A.; Kamali, S.; Häggström, L.; Gustafsson, T.; Thomas, J. O. *J. Mater. Chem.* **2006**, *16*, 2266.
(2) Dominko, R.; Bele, M.; Gaberšček, M.; Meden, A.; Remškar, M.; Jamnik, J. *Electrochem. Commun.* **2006**, *8*, 217.
(3) Dominko, R. *J. Power Sources* **2008**, *184*, 462.
(4) Sirisopanaporn, C.; Masquelier, C.; Bruce, P. G.; Armstrong, A. R.; Dominko, R. *J. Am. Chem. Soc.* **2011**, *133*, 1263.
(5) Armstrong, A. R.; Kuganathan, N.; Islam, M. S.; Bruce, P. G. *J. Am. Chem. Soc.* **2011**, *133*, 13031.
(6) Eames, C.; Armstrong, A. R.; Bruce, P. G.; Islam, M. S. *Chem. Mater.* **2012**, *24*, 2155.
(7) Liivat, A. *Solid State Ionics* **2012**, *228*, 19.
(8) Saracibar, A.; Van der Ven, A.; Arroyo-de Dompablo, M. E. *Chem. Mater.* **2012**, *24*, 495.
(9) Liivat, A. *Solid State Ionics* **2011**, *192*, 58.
(10) Kempaiah, D. M.; Rangappa, D.; Honma, I. *Chem. Commun.* **2012**, *48*, 2698.
(11) Devaraju, M. K.; Tomai, T.; Unemoto, A.; Honma, I. *RSC Adv.* **2013**, *3*, 608.
(12) Kokalj, A.; Dominko, R.; Mali, G.; Meden, A.; Gaberscek, M.; Jamnik, J. *Chem. Mater.* **2007**, *19*, 3633.
(13) Muraliganth, T.; Stroukoff, K. R.; Manthiram, A. *Chem. Mater.* **2010**, *22*, 5754.
(14) Mali, G.; Meden, A.; Dominko, R. *Chem. Commun.* **2010**, *10*, 3306.
(15) Kalantarian, M. M.; Asgari, S.; Mustarelli, P. *J. Mater. Chem. A* **2013**, *1*, 2847.
(16) Chen, Z.; Qiu, S.; Cao, Y.; Qian, J.; Ai, X.; Xie, K.; Hong, X.; Yang, H. *J. Mater. Chem. A* **2013**, *1*, 4988.
(17) Politaev, V. V.; Petrenko, A. A.; Nalbandyan, V. B.; Medvedev, B. S.; Shvetsova, E. S. *J. Solid State Chem.* **2007**, *180*, 1045.
(18) Arroyo-de Dompablo, M. E.; Armand, M.; Tarascon, J.; Amador, U. *Electrochem. Commun.* **2006**, *8*, 1292.
(19) Gummow, R.; Sharma, N.; Peterson, V.; He, Y. *J. Solid State Chem.* **2012**, *188*, 32.
(20) Aono, S.; Tsurudo, T.; Urita, K.; Moriguchi, I. *Chem. Comm* **2013**, *49*, 2939.
(21) Sun, W.; Cao, F.; Liu, Y.; Zhao, X.; Liu, X.; Yuan, J. *J. Mater. Chem.* **2012**, *22*, 20952.
(22) Rangappa, D.; Murukanahally, K. D.; Tomai, T.; Unemoto, A.; Honma, I. *Nano Lett.* **2012**, *12*, 1146.
(23) Perdew, J. P.; Burke, K.; Ernzerhof, M. *Phys. Rev. Lett.* **1999**, *77*, 3865.
(24) Dudarev, S. L.; Botton, G. A.; Savrasov, S. Y.; Humphreys, C. J.; Sutton, A. P. *Phys. Rev. B* **1998**, *57*, 1505.
(25) Monkhorst, H. J.; Pack, J. D. *Phys. Rev. B* **1976**, *13*, 5188.
(26) Zhang, P.; Hu, C. H.; Wu, S. Q.; Zhu, Z. Z.; Yang, Y. *Phys. Chem. Chem. Phys.* **2012**, *14*, 7346.
(27) Courtney, I. A.; Tse, J. S.; Mao, O.; Hafner, J.; Dahn, J. R. *Phys. Rev. B* **1998**, *58*, 15583.
(28) Aydinol, M. K.; Kohan, A. F.; Ceder, G.; Cho, K.; Joannopoulos, J. *Phys. Rev. B* **1997**, *56*, 1354.
(29) Giannozzi, P.; et al. *J. Phys.: Condens. Matter* **2009**, *21*, 395502.
(30) Clark, S. J.; Segall, M. D.; Pickard, C. J.; Hasnip, P. J.; Probert, M. J.; Refson, K.; Payne, M. C. *Z. Kristallogr.* **2005**, *220*, 567.
(31) Chen, Y.; Li, F.; Tang, D.-M.; Jian, Z.; Liu, C.; Golberg, D.; Yamada, A.; Zhou, H. *J. Mater. Chem. A* **2013**, *1*, 13076.
(32) Bruce, P. G.; Hardwick, L. J.; Abraham, K. M. *MRS Bull.* **2011**, *36*, 506.
(33) Abraham, K. M.; Jiang, Z. *J. Electrochem. Soc.* **1996**, *143*, 1.
(34) Visco, S. J.; Katz, B. D.; Nimon, Y. S.; Dejonghe, L. D. U.S. Patent 2007 7282295.